

# A Novel Automated Method for Analyzing Semen Microscopy Images: Curvelet Paradigm as a Solution for Improving Sperm Detection

Payam Taheri<sup>1</sup>, Seyed Vahab Shojaedini<sup>2\*</sup>

1. Faculty of Electrical, Biomedical and Mechatronics Engineering, Qazvin Branch, Islamic Azad University, Qazvin, Iran
2. Department of Biomedical Engineering, Iranian Research Organization for Science and Technology (IROST), Tehran, Iran.

## ARTICLE INFO

**Article type:**  
Original Paper

**Article history:**  
Received: Feb 16, 2021  
Accepted: Jun 11, 2021

**Keywords:**  
Microscopy Images  
Sperm Detection  
Curvelet Framework  
Nonlinear Mapping  
Function

## ABSTRACT

**Introduction:** Credible research shows that in many cases, infertility is caused by problems with men's sperm. Therefore, an accurate sperm analysis is a necessity to solve the problem of infertile couples. However, the first step in this analysis is to separate the sperm from the semen, which may not be accurate due to the poor contrast of the captured microscopy images.

**Material and Methods:** Curvelet transform has been introduced in recent years as an effective tool for object detection in the image processing domain. The most significant advantage of this transform is that it maps the raw image to a new space in which the features are sparser and parallelly more directional. Based on this fact, in this study, this approach is used to more effectively detect sperm in microscopic images. However, intelligent adjustment of the parameters of this mapping plays an important role in strengthening the weaker edges, and therefore in this article, a new method for optimizing the mapping parameters in order to achieve better separation of sperms from the background of the semen image is also proposed and examined.

**Results:** The comparison of the results obtained from examining the proposed method versus the results of the state of art methods was performed by using the two main criteria including sperm detection rate and false detection rate (i.e., false positives). This comparison clearly indicated the effectiveness of the proposed idea in distinguishing sperms from semen background. When the basis of performance evaluation is based on not detecting even a single false particle, it is observed that the correct sperm detection rate in the proposed method is between 4 and 17 percent higher than alternative methods. However, the false detection parameter itself shows an improvement of 33% to 3% in the proposed method compared to the weakest to the best among alternatives.

**Conclusion:** Investigating the ROC curve which has been obtained from several examinations showed the effectiveness of the proposed idea over its alternatives either in correct detection of sperms or elimination of false objects. Therefore, the obtained results may lead us to the conclusion that the curvelet transform may be utilized as an effective solution for detecting sperms in low contrast microscopic images of human semen.

### ► Please cite this article as:

Taheri P, Shojaedini V. A Novel Automated Method for Analyzing Semen Microscopy Images: Curvelet Paradigm as a Solution for Improving Sperm Detection. Iran J Med Phys 2022; 19: 115-124. 10.22038/IJMP.2021.55758.1924.

## Introduction

Infertility is a disease of the reproductive system which is defined as not being able to become pregnant after a year of regular sexual relationship [1, 2].

A considerable portion of infertility cases are caused by fertility problems in men, therefore one of the most important ways for the treatment of infertility is the semen analysis [3, 4]. The most important component of the semen are sperms which are male reproductive cells. Therefore, estimating sperm parameters (i.e., count, motility, morphology, volume, fructose level, and PH) may lead to determine the cause of infertility [5, 6]. Microscopic imaging is a new technique which has been widely used in recent decades which enabled infertility specialists to visually analyze the sperm behavior [7, 8].

However, the reliability of this technique is strongly dependent on the experience of the

technician therefore its effectiveness is hampered by the procedure of measurement and human errors. Additionally, this technique is so time-consuming. Based on these facts, automatic analysis of sperms has been substituted [9]. The most challenging problem in automated analysis is to distinguish sperms from other parts of semen specimen which is called sperm detection [9]. It is clear from the outset that the low quality of microscopic images of semen which is mainly due to the low contrast of such images is a significant problem, in addition, these images have been taken in different conditions, and it seems to be an inherent problem of such images. Unfortunately, this situation causes problems such as combining adjacent sperms or even fragmentation of other low contrast sperms, which is a serious problem for automated procedures and increases the false alarm

\*Corresponding Author: Tel: +982156276311; Email: shojadini@irost.ir

rate in parallel with decreasing the true positive rate. As result, the automated sperm detection in microscopy images has remained as an open problem. So far various methods have been proposed to solve the problem of sperm detection in microscopic images.

In a group of researches, some versions of thresholding methods have been applied in order to separate sperms from the background of images [10]. Although the simplicity of the thresholding concept may be considered as its most important advantage, the results are not favorable because non-sperm objects have the same intensity distribution as the sperms [10, 11].

Some other methods utilize prior information about the edge and shape of sperms for distinguishing them from other parts of semen. The obtained results show that this group of methods has a great ability in detecting heads of sperms which usually have stronger edges and more regular shapes. Unfortunately, the aforementioned techniques are not able to detect those sperms which have not enough lighting or the supposed head shape [12]. A group of methods endeavored to enhance the result of sperm detection by incorporating other algorithms which are focused on sperm movement [13]. Split-merge followed by K-nearest Neighborhood [14], the mean shift [15], and the optical flow (OF) algorithm which is based on the movement of their tails [16], are some important examples of this family of methods. The first two methods, despite their simplicity, have not shown acceptable performance, especially in removing false particles in the captured microscopic image [14-15]. On the other hand, the disadvantage of the optical flow technique is that its performance depends on the intensity of the sperm tail and its possible movements. However, in many cases, the tail area in sperm may be less clear and cohesive than the head region, which hampers the performance of OF technique in actual use [16]. As another member of this family, we can mention the Kalman filtering that has been improved by graph theory pruning, which has been introduced in some previous researches of authors [17]. The above methods essentially need to process the videos captured from the semen sample, which considerably increases the processing cost. In addition, significant decreases in performance of these methods are observed when they are applied to several semen videos in them either sperms have wide movement area or their tails have fast motions.

Some methods utilize the watershed segmentation concept as a basis for distinguishing sperms from other particles of the semen. As representatives of this type of method, we can refer to the two methods (i) watershed-based sperm detection modified by fuzzy entropy concept [18] and (ii) watershed-based sperm detection modified by graph theory concept [17], which both were presented in previous papers of the authors. Since watershed approaches are usually

directly implemented on pixels, the performance of this family of methods is so sensitive to the image contrast, which leads to relatively unreliable results in low contrast microscopic images [17-18].

In some recent studies, neural network-based methods have been applied in order to recognize sperms [19-20]. Although such methods sometimes lead to acceptable results in identifying sperms due to their learning process (e.g., especially in situations where their test and training data have significant similarities), like most learning-based methods, their performance is highly dependent on their training samples and therefore in different test conditions, do not lead to satisfactory outcomes.

In this work, we have devised a new approach for detecting sperms in the microscopy images. In the proposed approach, it is tried to obtain a better demonstration by using digital curvelet decomposition, which leads to a higher degree of orientational specifications. Furthermore, this approach obtains better handling of singularities in transformed microscopy image than the original image. In the next step, nonlinear mapping is applied to the curvelet sub-bands which magnifies the weak ridges of the sperms. The above procedure increases the chance of sperm detection compared to the raw image in which sperms are enclosed by non-magnified boundaries. In the last step, the sperm boundaries are determined by applying a watershed approach on the mapped image.

This article is arranged as follows. In part 2, our suggested method has started by evaluating the Unequally Spaced Fast Fourier Transform, which constructs the curvelet decomposition and has pursued the sperm extracting method at the end of this section. In Part 3, the results of our method for a variety of inputs have been reviewed. In part 4, the accomplished outcomes from the proposed method have been compared with the outcomes of some existing approaches by using appropriate frameworks. At the end part of this article, the conclusion has been mentioned.

## Materials and Methods

Suppose a captured microscopy image including  $A$  rows and  $B$  columns. Generally,  $I$  may be composed of sperms as well as other semen components which are called background in this article. At first, it is considered a two-dimensional space like  $Z^2$  which companies with  $r$  and  $\theta$  as polar coordinates. At the next step, it is considered a radial window like  $R(r)$  and an angular window like  $\Psi(\theta)$  which both of these windows have real positive domains and obey upcoming conditions [21]:

$$\sum_{j=-\infty}^{\infty} R^2(2^j r) = 1, \quad r \in (3/4, 3/2) \quad (1)$$

$$\sum_{l=-\infty}^{\infty} \Psi^2(\theta - l) = 1, \quad \theta \in (-1/2, 1/2) \quad (2)$$

In above-mentioned series,  $j$  represents scale and  $l$  represents an angular location. An example of these windows is shown in the figure (1).

Based on the above descriptions, a window may be defined as equation (3) for each  $j \geq j_0$  which  $j_0$  is related to the maximum curvature of the edge [22]:

$$Q_j(r, \theta) = 2^{-3j/4} R(2^{-j}r) \Psi\left(\frac{2^{lj/2} \theta}{2\pi}\right) \quad (3)$$

Now let rotation angles be defined as equation (4):

$$\left(\theta_l = 2\pi 2^{-\lfloor \frac{l}{2} \rfloor} l\right) \quad (4)$$

In which angular location  $l$  is considered in terms of scale  $j$ , as:

$$l = 0, 1, \dots, 2^j - 1 \quad (5)$$

Therefore, other curvelets may be obtained in polar space by rotating  $\theta_l$  at positions  $y_k^{j,l}$  and scaling by  $2^{-j}$  as below equation:

$$\xi_{j,l,k}(y) = \xi_j H_{\theta_l} \left( y - \left( H_{\theta_l}^{-1}(k_1 \cdot 2^{-j}, k_2 \cdot 2^{-j/2}) \right) \right) \quad (6)$$

For more simplicity the symbol  $k$  may be defined as  $k = (k_1, k_2) \in Z^2$ . In the equation (6),  $H_{\theta_l}$  is an operator which rotates by  $\theta$  radians and  $H_{\theta_l}^{-1}(k_1 \cdot 2^{-j}, k_2 \cdot 2^{-j/2})$  represents position parameters which are defined as  $y_k^{j,l}$ . Based on these parameters, the curvelet coefficients at each scale  $j$ , angular location  $l$ , and sequence  $k$  may be estimated by using equation (7). Furthermore, the sample scale view may be observed in figure (2).

$$CUR_{(j,l,k)}^c = \langle I, \xi_{j,l,k} \rangle = \int_{R^2} I(y) \overline{\xi_{j,l,k}(y)} dy \quad (7)$$

As a digital version of curvelet transform is necessary to implement the proposed scheme of this article, in order to obtain this format of coefficients, firstly the equations (6)-(7) are rewritten in their discrete form as below:

$$\xi_{j,l,k}^D(y) = 2^{3j/4} \xi_j^D \left( H_{\theta_l}(y - y_k^{j,l}) \right) \quad (8)$$

Which  $l = -2^{\lfloor j/2 \rfloor}, \dots, 2^{\lfloor j/2 \rfloor} - 1$  and  $\theta_l$  is defined as  $l \cdot 2^{-\lfloor j/2 \rfloor}$ . The symbol  $D$  implies to the digital form, furthermore  $H_{\theta}$  may be reformatted as:

$$H_{\theta} = \begin{pmatrix} 1 & 0 \\ -\tan(\theta) & 1 \end{pmatrix} \quad (9)$$

Now the digital format of curvelet transform may be computed for the main image  $I$  as:

$$CUR^D(j, l, k) = \sum_{0 \leq a' \leq A} \sum_{0 \leq b' \leq B} I[a', b'] \xi_{j,l,k}^D[a', b'] \quad (10)$$

The above computations may be performed by using Fast Fourier Transform (FFT) which leads to lower computational cost and higher speed in obtaining curvelet transform.

$$CR^D = IFFT \left( FFT(I[a', b']) \times FFT(\xi_{j,l,k}^D[a', b']) \right) \quad (11)$$

It is worth noting that in this paper the Unequally Spaced Fast Fourier Transform (USFFT) is utilized to estimate Fourier coefficients, based on using concentric circles with concentric squares as curvelet scale view in polar coordinate.

For microscopic images containing sperm particles, high magnification is needed due to the small size of the objects, but applying magnification has its own problems. For example, reducing the contrast of such images or even chromatic Aberrations that reduces the quality of images. In this study, an attempt was made to improve this and further detect sperm by using the Curvelet transform based on its better sparse representation and more directionality properties. A very effective advantage of using this transform is that by using the appropriate mapping functions on the resulting coefficients, a sharper image may be obtained than the raw image, without making use of expensive magnifier hardware. Therefore, curvelet transform may provide a more attractive solution in order to distinguish sperms in semen from its other particles.

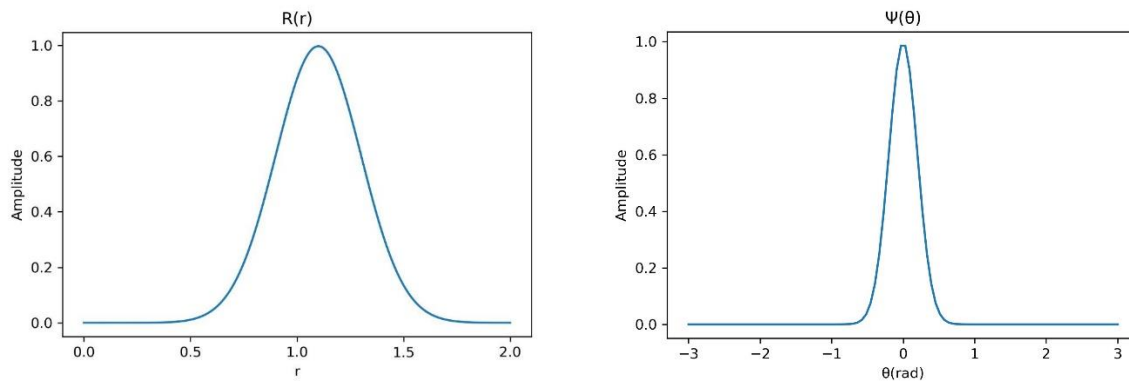


Figure 1. Examples for radial window  $R(r)$  and an angular window  $\Psi(\theta)$

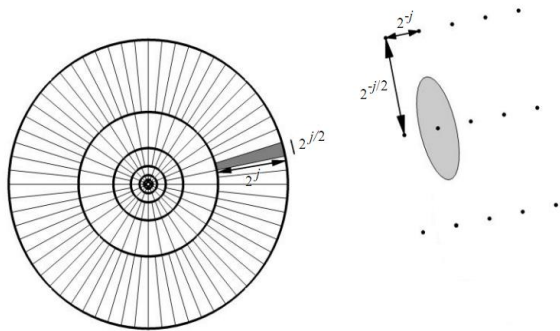


Figure 2. curvelet scale view in polar coordinate at left hand and space Cartesian grid at right hand

**Mapping Function**

Due to the poor contrast of microscopic images, in the second step of the proposed algorithm, a modification function is applied to the curvelet coefficients. This function changes the curvelet coefficients in such a way that the modified image (i.e.,  $I_c$ ) has a better contrast compared to the original image. The modification function makes use of a nonlinear logic until data of the small amplitude are enlarged at the expense of the larger ones, furthermore, it tries to perform this task uniformly over all scales. The main parameters of the nonlinear function are defined based on statistical features of curvelet coefficients. This strategy for parameter estimating makes the performance of the mapping function which is defined as equation (12), more consistent with the nature of the microscopic image, which leads to the more sharpened image.

$$f(v) = \begin{cases} w_1 \left(\frac{t}{s}\right)^e & \text{if } |v| < rs \\ w_2 \left(\frac{a}{v}\right)^x & \text{if } rs \leq |v| < t \\ w_3 & \text{if } t \leq |v| \end{cases} \quad (12)$$

In the above equation  $e, x$  are nonlinearity degrees and may take values in the range of  $[0 \ 1]$ , in addition,  $v$  demonstrates primary curvelet coefficients. Furthermore,  $w_1, w_2$  and  $w_3$  represent weights related to each criterion of  $f(v)$  and cause more directional magnification which may lead to better control and modification. The symbol  $r$  is used to regulate the coefficient modification interval. Parameters  $s, t$  are defined according to some specifications of the curvelet coefficient to provide interval modification and regulate the amplitude of the corresponding function. In order to modeling of noise and subsequently try to remove it,  $s$  is defined as noise standard deviation at a special scale  $j$  and direction  $l$  [23]. In the process of implementation and evaluation, it was found that the modification of coefficients and consequently, the effectiveness of the proposed method depends on the parameters of the mapping function. Thus, with the trial-and-error

strategy, an attempt was made to obtain the best parameters. In the above investigations, parameters  $t, a$  are defined as  $t = h_1 m$  and  $a = h_2 t$  while  $h_1, h_2$  are independent. Finally,  $m$  demonstrate the maximum value among curvelet coefficients. Description of parameters is summarized as shown in Table (1).

Table 1. Main parameters of modification function

Parameters	Values	Parameters	Values
$e$	0.1	$w_1 = w_2$	1
$h_1$	0.3	$w_3$	1
$h_2$	4	$r$	17

The effect of the parameters of the modification function has been demonstrated in figure (3). This figure describes the quality of modification according to different values of  $e, x$  and by setting  $t = 30, r = 17$ . Investigation of the performance of the mapping function may demonstrate that increasing  $e, x$  between zero and about 0.14 makes a good effect on coefficients without almost any distortion in the output image while choosing  $e, x$  in (0.14-0.5) made more magnification but a little distortion in output image may happen. Furthermore, defining values in the range of (0.5-1) makes the highest magnification but much more distortion (redundancy) may have occurred. Finally, values more than 1 are not suitable in practice because of their damaging effect on the transformed image which causes the background will be bolded too.

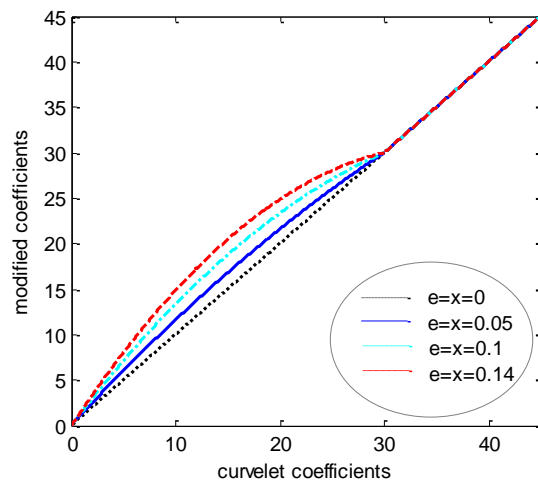


Figure 3. Performance of mapping function according to changes of its parameters

**Extracting sperms**

In the final step of the proposed algorithm, the sperms are detected among  $I_c$  (i.e. the modified image resulted from section 2-2). For this purpose,  $\Delta I_{c,\min}$  is constructed as a set of  $G$  local minimums of  $I_c$ ,

furthermore each member of  $\Delta I_{c,\min}$  may be considered as a single object like  $V'_{g'}$ , as:

$$\Delta I_{c,\min} = \{V'_1, \dots, V'_{g'}, \dots, V'_{G'}\} \quad (13)$$

In which:

$$V'_{g'} = \{1 \leq a \leq A, 1 \leq b \leq B | I_{c,ab} = \min(W_{ab})\} \quad (14)$$

In above equation,  $W_{ab}$  is a window which is centered at a location  $(a, b)$ . The intensity of the center is  $I_c(a, b)$  which is shown by using symbol  $\eta$  for brevity in rest of this section.

The neighbors of each member of  $\Delta I_{c,\min}$  may be considered as either extension of an existing object (i.e.,  $V'_{g'}$ ) or a new object. To assign each neighbor to one of existing set of sperms, firstly the geodesic influence zone of  $\Delta I_{c,\min}$  is updated as below equations [17-18, 24]:

$$\Omega(\Delta I_{c,\min}) = \cup_{g'} \Omega'(V'_{g'}, \Delta I_{c,\min}) \quad (15)$$

In which  $\Omega'(V'_{g'}, \Delta I_{c,\min})$  is defined as:

$$\Omega'(V'_{g'}, \Delta I_{c,\min}) = \{a, b | sc(I_{c,ab}, V'_{g'}) < \varepsilon, sc(I_{c,ab}, V'_{g''}) < sc(I_{c,ab}, V'_{g'})\} \quad (16)$$

If  $\tau_\eta$  is supposed as the set of all local minimums at gray level  $\eta$  who are not assigned to any sperm (i.e. remained candidates), then the set of sperms should be started from  $\eta_{\min}$  (i.e. lowest gray level) as below:

$$\Delta I_{c,\min+1} = \Delta I_{c,\min} \cup \Omega(\Delta I_{c,\min}) \cup \tau_{\min} \quad (17)$$

The above set is expanded sequentially by increasing the gray level as:

$$\Delta I_{c,\eta+1} = \Delta I_{c,\eta} \cup \Omega(\Delta I_{c,\eta}) \cup \tau_\eta \quad (18)$$

By sequential recursion of equation (18) the set of objects may be expanded by assigning higher level pixels as below equations:

$$\Delta_{(\eta+1)} = \Delta_\eta \cup \Omega(\Delta_\eta) \cup \tau_{(\eta+1)} \quad (19)$$

In which:

$$\Omega(\Delta_\eta) = \cup_{g'} \Omega'(V'_{g'}, \Delta_\eta) \quad (20)$$

Table 2- Specifications of test frames

Specification	Value	Specification	Value
Sperm size	30-50 pixels	Number of frames	3480
Frame size	480×720 pixels	Speed of sperms	0-2 pixels per frame
Video frame rate	29 fps	Average contrast	23
Number of persons	11 persons	Density of sperm per milliliter	> 2×10 <sup>6</sup>
Number of videos	11	Age of examined persons	22-35 years old

It is clear that  $\Omega'(V'_{g'}, \Delta_\eta)$  is computed by equation (16). The above procedure proceeds to the highest brightness level, until  $\Delta I_{c,\max}$  is constructed as the final set of sperms as:

$$\Delta I_c = \Delta I_{c,\max} = \{V_1, \dots, V_g, \dots, V_G\} \quad (21)$$

In which  $V$  is a set of  $G$  final objects which are captured from  $I_c$ . The Flowchart of the proposed method has been shown in figure (4).

## Results

The proposed algorithm was applied to various videos obtained from semen microscopy. The data set was captured by an Orca ER Digital CCD Camera mounted on a Nikon invert microscope using a 40x zoom lens. The specifications of the data set are presented in Table (2).

So far, several methods have been proposed to improve the quality of images. The purpose of some of these methods is to visually enhance the image and the purpose of others is to improve the separation of image elements. Based on the above descriptions some criteria have been introduced so far to quantify the desired improvement. It is important that in cases similar to our application the improvement is not merely the target but the improvement of the image only as an introduction to subsequent processes (e.g., particle detection). Consequently, in these applications, the best evaluation parameter is the effect of the proposed image improvement scheme on the final results (i.e., detection statistics).

Based on the above strategy, the proposed method was implemented by using MATLAB 2013a along with Zernike moments Algorithm (ZMA) up to 10<sup>th</sup> order of moments [25], Watershed Segmentation Algorithm (WSA) [26] and Morphological Contour Synthesis (MCS) [27] to be compared with one another. An important feature of these methods is that all of them have been proposed and implemented in the authors' researches in recent years and their superiority over the existing classical methods has been shown [25-26-27]. The captured videos were first processed manually by an expert in order to obtain a ground truth to compare the automatic methods with. Then, sperms were detected by applying the proposed method and its three alternatives. Finally, the performance of each algorithm was determined by comparing its results with manual detection results as ground truth.

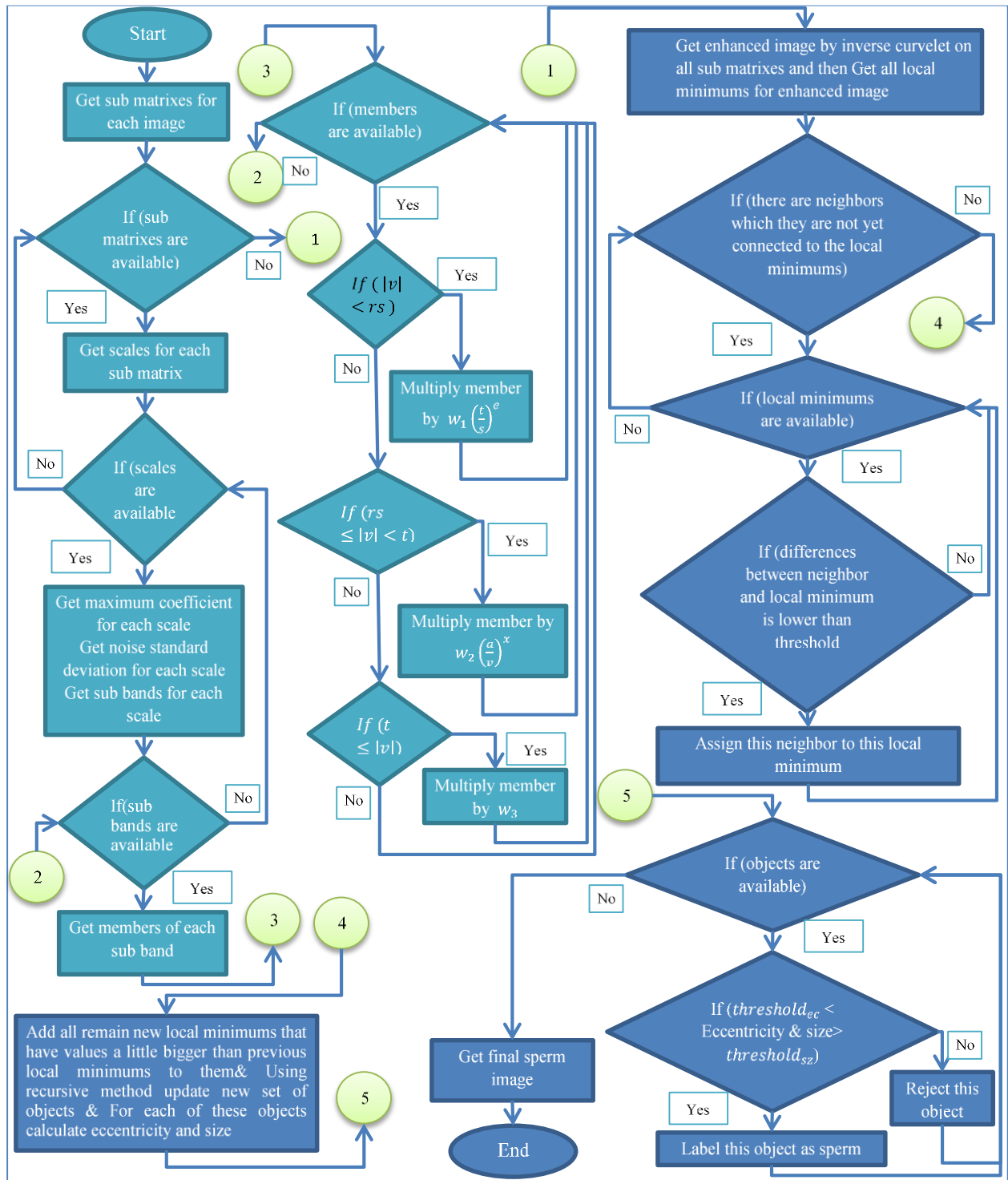
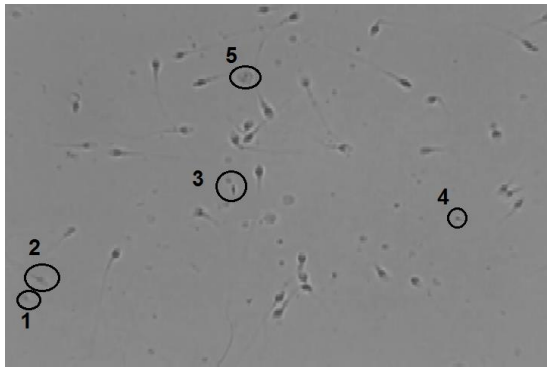


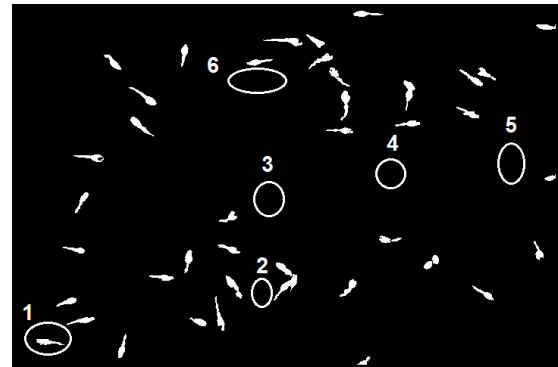
Figure 4. Flowchart of the proposed method

Two samples of the examined frames were exhibited in figures (5-a, 5-f). The rest of figures illustrate the performance of the proposed, ZMA, WSA and MCS methods on the above samples. Figure (5-b) shows that the proposed method has extracted all (i.e. 37 sperms) which had been presented in figure (5-a) in parallel with three false detections. In a similar manner, figure (5-g) displays

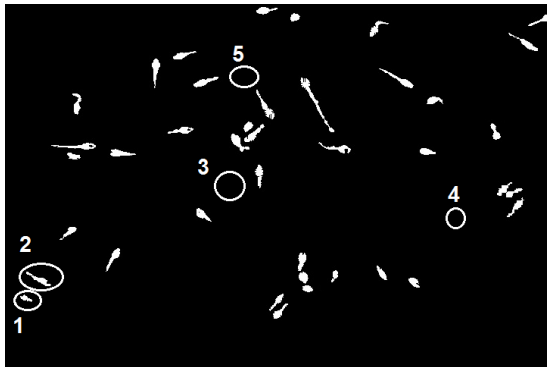
that the proposed method has extracted 41 of 42 sperms that were shown in figure (5-f) with just two false detections. Figures (5-c) and (5-h) show the results of applying ZMA on the contents of figures (5-a) and (5-f), respectively.



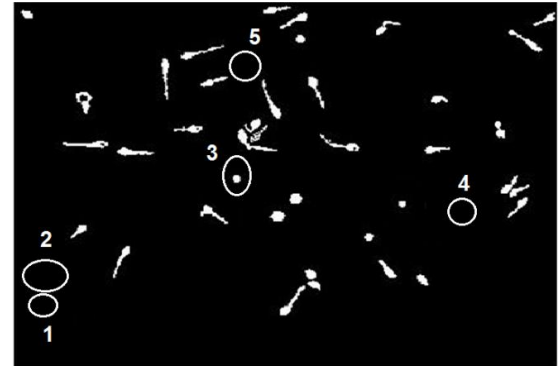
4(a)



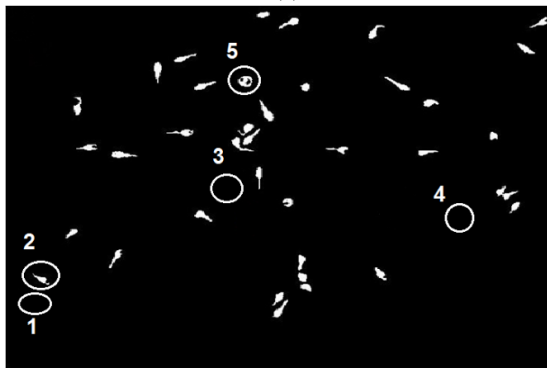
4(g)



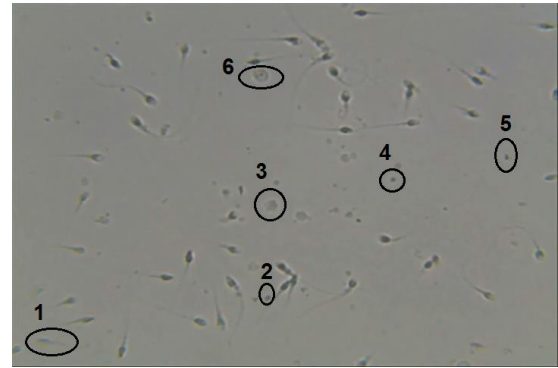
4(b)



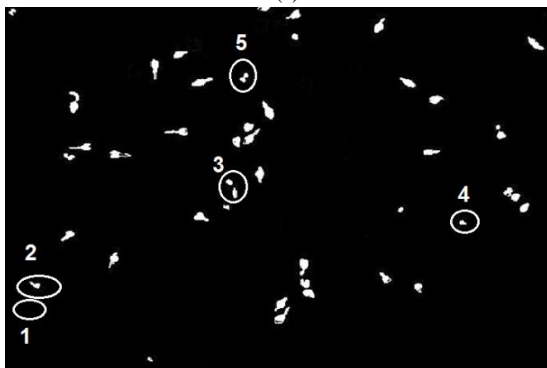
4(d)



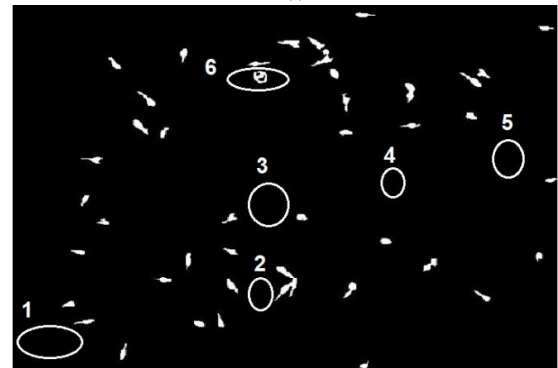
4(c)



4(f)



4(e)



4(h)

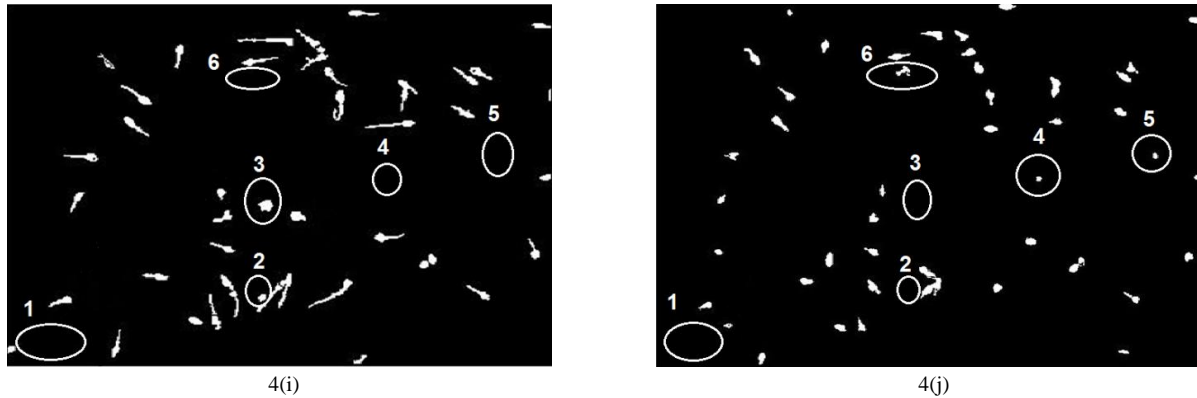


Figure 5. (a, f) the original frames and the results of detection by using (b, g) proposed method, (c, h) ZMA, (d, i) WSA, (e, j) MCS algorithm

These figures show that ZMA has extracted 34 and 40 sperms correctly from the mentioned reference images, respectively in parallel with 4 and 6 false detections. The obtained results from applying the watershed method may be observed in figures (5-d) and (5-i). These figures indicated that the above method has extracted 31 and 37 sperms correctly from the reference images (5-a) and (5-f), in parallel with 8 and 7 false detections, respectively. Figure (5-e) demonstrates that the third alternative algorithm (i.e., MCS) has extracted 34 sperms correctly from the reference image (5-a). Similarly, figure (5-j) demonstrates that this algorithm has extracted 39 sperms correctly from the image (5-f). These results were obtained when false detections of 10 and 8 occurred for each of the above frames, respectively. The mentioned results indicated that the proposed method had a higher ability either in detecting sperms or rejecting non-sperm objects than existing methods, as follows. For example, in figure (5-a), three non-sperm particles were marked as “3”, “4” and “5” which might be confused with the sperms because of their contrasts and shapes. Figure (5-b) demonstrates that the proposed algorithm rejected all three non-sperm particles, whereas the alternative methods (i.e., ZMA, WSA, and MCS) have considered some or all of them as sperms, as have been marked in figures (5-b), (5-c) and (5-d). Furthermore, in figure (5-a), objects “1” and “2” showed low contrast sperms which might be loosed by automatic methods because of their poor contrast. Figure (5-b) illustrates that object “1” was detected as a correct sperm by the proposed algorithm while none of the alternative methods (i.e., ZMA in figure (5-c), WSA in figure (5-d) and MCS in figure (5-e)) were not able to detect this low contrast sperm.

Another, example may be observed in figures (5-f) to (5-j). Figure (5-f) displays sperm and non-sperm objects of the second example frame in such a way the sperm has been marked as “1”, as well as non-sperm objects which have been marked as “2-6”. Figure (5-g) demonstrates that the proposed method detected sperm “1” correctly while removing all none sperm objects. Figure (5-h) demonstrates that ZMA not only could not detect sperm “1” but also falsely detected “6” as sperm. Figure (5-i) shows that WSA missed sperm “1” just like ZMA and has wrong results about “2” and “3” in such way that it has

marked both of them as sperm. Last Figure (i.e. figure (5-j)) demonstrates the results of applying MCS algorithm which rejects sperm “1” in parallel with obtaining three false detections “4”, “5”, and “6”.

## Discussion

Real data which had been obtained from semen microscopy were processed by using the proposed algorithm and its alternatives including ZMA, WSA, and MCS algorithms. The obtained results were evaluated based on two standard parameters in detection literature which have been described in equations (22-23). Equation (22) computes True Positive Rate (*TPR*) which demonstrates the rate of truly identified sperms over all sperms.

$$TPR = \frac{TP}{(TP+FN)} = \frac{TP}{P} \quad (22)$$

In which *TP* and *FN* denotes correct and false detected sperms, respectively.

The next formula computes False Positive Rate (*FPR*) which illustrates the rate of objects which have been falsely detected as sperms over sum of the true rejected non-sperms objects and false detected objects.

$$FPR = \frac{FP}{(FP+TN)} = \frac{FP}{N} \quad (23)$$

In which *FP* and *TN* denote false positives and true negatives respectively.

In fact, these two criteria demonstrate useful information about two main types of errors in sperm detection application. The *TPR* (i.e., recall) indicates what ratio of the sperms has been detected correctly, and therefore the complement of this parameter (i.e.,  $1-TPR$ ) demonstrates the amount of unnecessary removal of the correct sperms. The second parameter (i.e., *FPR*) indicates how many of the incorrect particles are mistakenly detected as sperms. These are the two most important errors that we face in sperm detection application, and based on this, they are practically the basis of the rest of our analysis in the continuation of the article.

By using the above parameters, ROC curves were calculated for the four investigated methods. Figure (6) shows changes in *TPR* versus *FPR* which indicate that the proposed method outperformed the three alternatives in such manner as discussed below.

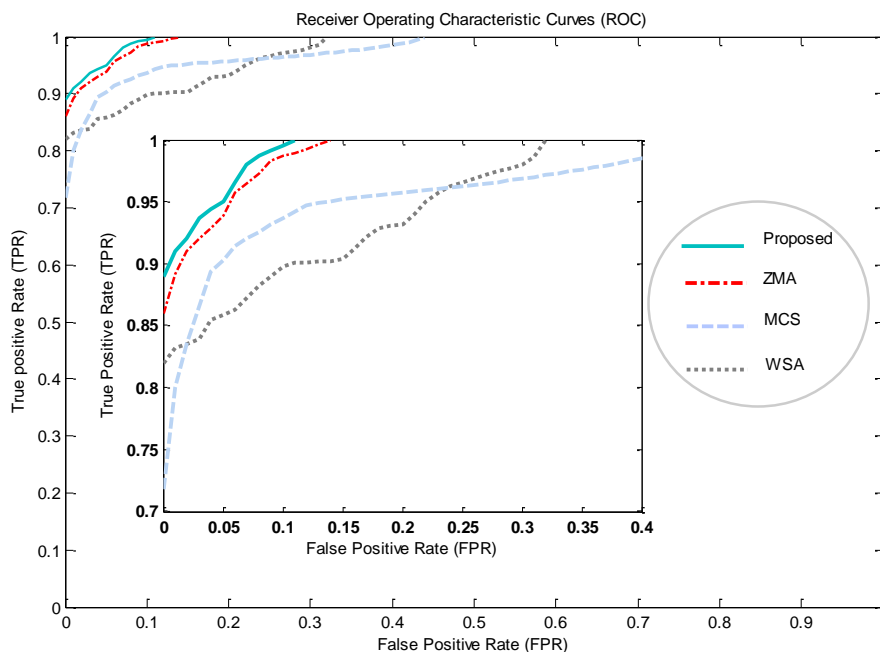


Figure 6. Demonstration of ROCs obtained for the examined algorithms

Table 3- Comparison of performances of examined algorithms

Parameters	performance of algorithms (%)			
	Proposed	ZMA	WSA	MCS
Detection rate against 0% false alarm	89	85	82	72
False detection rate against 100% detection	11	14	32	44

For better interpretation of ROC results,  $FPR=0\%$  and  $TPR=100\%$  were considered as ideal values for false and true detections, then table (3) was constructed using these extremes of figure (5). This table shows that in  $FPR=0\%$ , the proposed algorithm has shown 4%, 7% and 17% superiority against ZMA, WSA and MCS algorithms, respectively. At another extreme (i.e.,  $TPR=100\%$ ), the proposed algorithm showed 3%, 21% and 33% superiority compared to ZMA, WSA and MCS algorithms, respectively.

### Conclusion

In the analysis of microscopic images of human semen, due to the very small size of sperm as the favorite particles in these images, it is necessary to use high magnification optical instruments. Using such equipment, in addition to creating the desired magnification, unfortunately also creates some problems. As one of the most important limitations, lens errors are an unfortunate problem caused by artifacts arising from the interaction of light with glass lenses even in modern optical microscopy which seriously degrades the quality of captured microscopic images. On the other hand, the considerable cost of such equipment is another limitation that hampers their use in microscopic imaging of semen. Accordingly, image processing methods with the aim of better detecting sperm than other particles in semen have been the focus of attention. Although several types of research have been performed so far, the two challenges of missing

correct sperms and extracting false particles have been the most important limitations that most of the proposed methods have faced. In this study, a new method was introduced for improving the above-mentioned parameters in detecting sperms in microscopic images. The proposed algorithm used the concept of sharpening the microscopic image by applying the optimized mapping function in the curvelet domain in order to overcome the above challenges in distinguishing low contrast sperms from other semen parts. To evaluate the performance of the proposed algorithm, it was examined on real microscopic images in parallel with three existing methods (i.e., ZMA, WSA, and MCS). Then, the obtained results were interpreted based on their ROCs. The results clearly demonstrated the superiority of the proposed method over alternatives either in the correct detection of sperms or the elimination of false objects. Results showed that the proposed algorithm distinguished sperms from other semen parts at least 4 percent better than its closest alternative in the presence of any false detection (i.e.  $FPR=0$ ). In addition, it was shown that the FPR of the proposed algorithm showed at least 3 percent improvement over the same method in the situation of full detection (i.e.,  $TPR = 100\%$ ). Based on the mentioned results, it may be concluded that the proposed method has a considerable potential to be used as a suitable tool for detecting sperms in low contrast microscopic images which have been captured from human semen.

## References

- Ortiz A, Simmons A, Gross A. Infertility: Secrets, Struggles, and Successes. Wise Women Book Collective. 2021.
- Evan R, Eaton J. Management of Infertility, Agency for Healthcare Research and Quality. 2019.
- Kumar R, Singh P. Prevalence and management of infertility in males with GUTB. BJUI Knowledge. 2020.
- Satashree P. Oxidative Stress: A Cause of Male infertility. Science Repository. 2020.
- Softness KA, Trussler JT, Carrasquillo RJ. Advanced sperm testing. Current Opinion in Urology. 2020 May 1;30(3):290-5.
- Garrido N, Rivera R, editors. Practical Guide to Sperm Analysis: Basic Andrology in Reproductive Medicine. CRC Press; 2017 May 25.
- Marc AF, Guppy JL, Bauer P, Mulvey P, Jerry DR, Paris DB. Validation of advanced tools to evaluate sperm function in barramundi (*Lates calcarifer*). Aquaculture. 2021 Jan 30;531:735802.
- Opstad IS, Popova DA, Acharya G, Basnet P, Ahluwalia BS. Live-cell imaging of human spermatozoa using structured illumination microscopy. Biomedical Optics Express. 2018 Dec 1;9(12):5939-45.
- Mahdavi HS, Monadjemi A, Vafae A. Sperm detection in video frames of semen sample using morphology and effective ellipse detection method. Journal of medical signals and sensors. 2011 Jul;1(3):206.
- Susrama IG, Purnama KE, Purnomo MH. Automated analysis of human sperm number and concentration (oligospermia) using otsu threshold method and labelling. In IOP Conference Series: Materials Science and Engineering 2016 (Vol. 105, No. 1, p. 012038). IOP Publishing.
- Xuan ZL, Yan WZ. The sperm video segmentation based on dynamic threshold. In 2010 International Conference on Machine Learning and Cybernetics 2010 Jul 11 (Vol. 5, pp. 2444-2448). IEEE.
- Nafisi VR, Moradi MH, Nasr-Esfahani MH. Sperm identification using elliptic model and tail detection. World Academy of Science, Engineering and Technology. 2005 Jun;6:205-8.
- Shojaedini SV, Goldar A, Soori M. Correntropy based sperm detection: a novel spatiotemporal processing for analyzing videos of human semen. Health and Technology. 2018 May;8(1):151-8.
- Abbiramy VS, Shanthi V, Allidurai C. Spermatozoa detection, counting and tracking in video streams to detect asthenozoospermia. In 2010 International Conference on Signal and Image Processing 2010 Dec 15 (pp. 265-270). IEEE.
- Tan WC, Mat Isa NA, Mohamed M. Automated human sperm tracking using mean shift-collision detection and modified covariance matrix method. Multimedia Tools and Applications. 2020 Oct;79(39):28551-85.
- Leung C, Lu Z, Esfandiari N, Casper RF, Sun Y. Detection and tracking of low contrast human sperm tail. In 2010 IEEE International Conference on Automation Science and Engineering. 2010 Aug 21 (pp. 263-268). IEEE.
- Shojaedini SV, Heydari M. A new method for sperm characterization for infertility treatment: hypothesis testing by using combination of watershed segmentation and graph theory. Journal of medical signals and sensors. 2014 Oct;4(4):274.
- Shojaedini SV, Heydari M. A New Method for Sperm Detection in Infertility Cure: Hypothesis Testing Based on Fuzzy Entropy Decision. Journal of Electrical and Computer Engineering Innovations (JECEI). 2014 Jul 1;2(2):69-76.
- Somasundaram D, Nirmala M. Faster region convolutional neural network and semen tracking algorithm for sperm analysis. Computer Methods and Programs in Biomedicine. 2021 Mar 1;200:105918.
- Rahimzadeh M, Attar A. Sperm detection and tracking in phase-contrast microscopy image sequences using deep learning and modified csr-dcf. arXiv preprint arXiv:2002.04034. 2020 Feb 11.
- Lang S, Liu X, Zhao B, Chen X, Fang G. Focused synthetic aperture radar processing of ice-sounding data collected over the east antarctic ice sheet via the modified range migration algorithm using curvelets. IEEE Transactions on Geoscience and Remote Sensing. 2015 Feb 24;53(8):4496-509.
- Candès EJ, Donoho DL. New tight frames of curvelets and optimal representations of objects with piecewise C2 singularities. Communications on Pure and Applied Mathematics: A Journal Issued by the Courant Institute of Mathematical Sciences. 2004 Feb;57(2):219-66.
- Zhao ZB, Yuan JS, Gao Q, Kong YH. Wavelet image de-noising method based on noise standard deviation estimation. In 2007 International Conference on Wavelet Analysis and Pattern Recognition 2007 Nov 2 (Vol. 4, pp. 1910-1914). IEEE.
- Roerdink JB, Meijster A. The watershed transform: Definitions, algorithms and parallelization strategies. Fundamenta informaticae. 2000 Jan 1;41(1, 2):187-228.
- Arkanfari R, Shojaedini SV. A new method for detecting sperms in microscopy images: combination of zernike moments and spatial processing. Iranian Journal of Medical Physics. 2018;15(4):215-21.
- Shojaedini SV, Heydari M. Automatic sperm analysis in microscopic images of human semen: Segmentation using minimization of information distance. Iranian Journal of Medical Physics. 2014;11(Issue):284-93.
- Arkanfari R, Shojaedini SV. A new method for detecting sperms in microscopy images: combination of zernike moments and spatial processing. Iranian Journal of Medical Physics. 2018;15(4):215-21.